Human Molecular Genetics, 2005, Vol. 14, No. 6 ***813–825***
doi:10.1093/hmg/ddi075
Advance Access published on February 9, 2005

Defective sister-chromatid cohesion, aneuploidy and cancer predisposition in a mouse model of type II Rothmund–Thomson syndrome

Michael B. Mann[1,2], Craig A. Hodges[1], Ellen Barnes[1,2], Hannes Vogel[3], Terry J. Hassold[1] and Guangbin Luo[1,2,*]

[1]Department of Genetics, Case Western Reserve University, Cleveland, OH 44106, USA, [2]Case Comprehensive Cancer Center, University Hospitals of Cleveland, Cleveland, OH 44106, USA and [3]Department of Pathology, Stanford University Medical Center, Stanford, CA 94305, USA

Received December 17, 2004; Revised and Accepted January 25, 2005

Type II Rothmund–Thomson syndrome (Type II RTS) is a rare autosomal recessive genetic disorder characterized by a congenital skin rash, birth defects of the skeleton, genomic instability and cancer predisposition. It is caused by mutations in the *RECQL4* gene and thus represents one of the three cancer-prone genetic diseases that are caused by mutations in a RecQ helicase-encoding gene. Genomic instability has been suspected as a major underlying cause of this disease, and analyses of Type II RTS patient-derived cells demonstrate unusually high frequencies of chromosomal aberrations, suggesting the involvement of chromosomal instability. However, the nature of the instability induced by *RECQL4* mutations has not been clearly defined. We created a viable *Recql4* mutant mouse model. These mice exhibit a distinctive skin abnormality, birth defects of the skeletal system, genomic instability and increased cancer susceptibility in a sensitized genetic background. Thus, they provide a useful model for studying Type II RTS. In addition, we demonstrate that cells from these mutant mice have high frequencies of premature centromere separation and aneuploidy. Thus, our observations provide evidence for a previously unsuspected role for Recql4 in sister-chromatid cohesion, and suggest that the chromosomal instability may be the underlying cause of cancer predisposition and birth defects in these mutant mice.

INTRODUCTION

Aneuploidy is a hallmark of most classes of solid tumors (1–4). The fidelity of segregating chromosomes, required for maintenance of euploidy, is facilitated by cell cycle checkpoints, particularly the mitotic spindle checkpoint (5–7). Prior to anaphase initiation, tension produced by the bipolar attachment of microtubules to the centromeres of paired sister-chromatids is required (5,8). Therefore, sister-chromatid cohesion has an essential role in establishing this bipolar attachment (9,10).

RecQ DNA helicases are an evolutionary conserved family of enzymes that share a seven-motif helicase domain (11). In both budding and fission yeast, null mutants of the single *RecQ* DNA helicase gene, *sgs1* and *rqh1*$^+$, respectively, exhibit hyper-recombination and chromosome mis-segregation (12–16). The chromosome mis-segregation phenotype of these mutants provided the first genetic evidence for a link between *RecQ* DNA helicases and chromosome segregation. Unlike unicellular organisms which have a single *RecQ* DNA helicase, mammals have five genes that encode different RecQ DNA helicases. For example, humans have *RECQL4*, *RECQL*, *BLM*, *WRN* and *RECQL5* (17,18). Loss-of-function mutations in *WRN*, *BLM* and *RECQL4* cause the autosomal recessive disorders Bloom (BS), Werner (WS) and Type II Rothmund–Thomson (Type II RTS) syndromes, respectively (19–21). Genomic instability and cancer susceptibility are common features of all three disorders, but the nature of the instability and tumor profiles vary among these syndromes. *WRN* deficiency results in large chromosomal deletions (22) and an increased susceptibility to malignancies, particularly sarcomas (23), whereas *BLM* deficiency leads to

*To whom correspondence should be addressed at: Department of Genetics, Case Western Reserve University, BRB 7th Floor, 10900 Euclid Avenue, Cleveland, OH 44106, USA. Tel: +1 2168447050; Fax: +1 2163683432; Email: gxl35@case.edu

elevated rates of crossovers in mitotic cells and increased susceptibility to all types of cancers observed in the general population (24). However, neither *WRN* nor *BLM* deficiency leads to defective mitotic chromosome mis-segregation or aneuploidy.

Type II RTS is a rare autosomal recessive genetic disorder characterized by a congenital skin rash, birth defects of the skeleton, genomic instability and increased susceptibility to malignancy, particularly early-onset osteosarcoma (25–30). Chromosome analyses of Type II RTS patient-derived cell cultures demonstrate unusually high frequencies of chromosomal instability (29,31–34), suggesting that RECQL4 may have a role in chromosome segregation. However, the nature of the instability induced by *RECQL4* mutations has not been established.

We report using gene targeting to generate a viable mouse model of Type II RTS. These mutant mice recapitulate the major phenotypes found in Type II RTS patients and hence provide a useful mouse model for delineating the mechanism(s) which contribute to the Type II RTS phenotype. *Recql4*$^{-/-}$ cells, derived from these mice, are aneuploid. We demonstrate that the aneuploidy phenotype is due to a defect in sister-chromatid cohesion. These findings reveal an important role of Recql4 helicase in sister-chromatid cohesion and mitotic chromosome segregation, and provide new insights into the link between chromosomal instability, birth defects and cancer predisposition.

RESULTS

Generation of a mouse model of Type II RTS by gene targeting

A majority of Type II RTS patients have *RECQL4* mutations that are predicted to result in the production of truncated polypeptides lacking an intact helicase domain (28), indicating that the RecQ helicase domain in RECQL4 is essential for its role in maintaining genome stability and suppressing cancer. Thus, we used gene targeting in mouse ES cells to generate a mouse model carrying a mutant *Recql4* allele that lacks an intact RecQ helicase domain. We replaced a 1075 bp fragment spanning from within exon 9 through exon 13 of the *Recql4* gene and encoding the conserved helicase domain (35), with a *PGKHprt* mini-gene (Fig. 1A).

Heterozygous mice carrying the *Recql4* mutant allele (designated *Recql4*^{tm1Glu} *or Recql4*$^{-}$) were readily obtained (Fig. 1B) and were indistinguishable from their wild-type siblings (data not shown). Matings between heterozygous mutant mice yielded the expected Mendelian ratios of wild-type, heterozygous and homozygous mutant offspring (data not shown). Southern blotting confirmed that the 1075 bp fragment between exon 9 and 13 was deleted from the genome of homozygous mutant mice (Fig. 1C). Accordingly, RT–PCR analysis also revealed that cells from these homozygous mutant mice did not express any wild-type *Recql4* transcript, but did express three major aberrant transcripts (Fig. 1D). Sequence analysis showed that all three contain exon 1 through 8 of the normal *Recql4* transcript followed by one of two cryptic exons from within the *PGK* promoter of the *PGKHprt* cassette. These cryptic exons contain in-frame

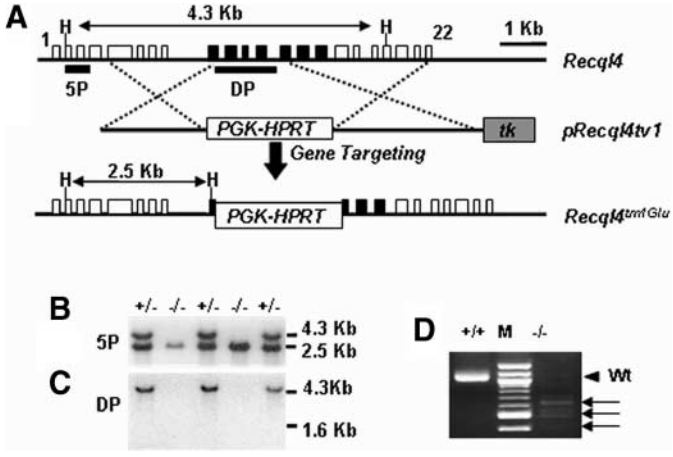

Figure 1. Generation of *Recql4* Knockout mice by gene targeting. (**A**) Schematic of the gene targeting strategy. The solid lines and boxes represent the intron and exon sequences, respectively. The exons that encode the conserved *RecQ* DNA helicase domain are shown as black boxes. The targeting construct, *pRecql4tv1*, was designed such that upon gene targeting a 1075 bp genomic fragment from within exon 9 to within exon 13 is replaced with a *PGKHprt* mini-gene cassette, resulting in the deletion of 80% of the genomic DNA that encodes the helicase domain. A correct targeting event converts a 4.3 kb *Hin*dIII fragment of the *Recql4* gene into a 2.5 kb *Hin*dIII fragment which can be detected by Southern blotting using the 5′ external probe (5P). (**B**) Identification of mice carrying the targeted *Recql4* mutant allele by Southern blotting. Genomic tail DNA was digested with *Hin*dIII followed by Southern blotting with the 5′ external probe. (**C**) Confirmation of the deletion in homozygous *Recql4* knockout mice by Southern blotting. The same membrane used in (B) was stripped and re-hybridized with a probe within the deleted region (DP). Note the loss of signal from lanes with DNA from homozygous mutant mice. (**D**) Detection of *Recql4* expression by RT–PCR. A pair of primers corresponding to exon 8 and exon 15 that flank the deleted region was used in the RT–PCR reactions. Total RNA isolated from mouse testis was used. Note that the RT–PCR product expected from normal *Recql4* transcript was amplified from RNA from the wild-type, but not from the *Recql4* homozygous mutant mouse (arrow head). Instead, three unexpected products (arrows) were amplified from RNA isolated from a *Recql4* homozygous mutant mouse. P*GK*, phosphoglycerate kinase promoter; *Hprt*, hypoxanthine-guanine phosphoribosyltransferase; *tk*, thymidine kinase gene; H, *Hin*dIII.

stop codons with respect to the normal *Recql4* open-reading frame. Therefore, all three aberrant transcripts are expected to produce either one of the two truncated polypeptides consisting of the N-terminal 480 amino acids of Recql4 plus 13 or 15 additional amino acids (either G M F V S S S L L N A N Q or A R V V Q D V T N G S S T S H) instead of the 1216 amino acids wild-type protein (35) or no protein products because of nonsense-mediated mRNA decay. These data confirm that the *Recql4*^{tm1Glu} mutant allele is similar to those *RECQL4* mutations identified in Type II RTS patients whose transcripts are expected to produce either no proteins or truncated polypeptides lacking the conserved helicase domain (28).

Although all homozygous mutant mice were born alive, 16% (50/314) of them died prior to 24 h of age, a significant increase in perinatal lethality when compared with the 4% (8/189) observed in control (wild-type and heterozygous) littermates ($\chi^2 = 16.09$, $P = 0.003$). We have not yet determined the precise cause(s) of death for these mice.

The remaining 84% of homozygous *Recql4* knockout mice were able to survive to adulthood and grew at similar rates as compared to wild-type littermates (data not shown). However, they displayed defects of the skin and skeleton, consistent with the organ systems affected in Type II RTS patients. Specifically, by 12 months of age, all homozygous mutant mice spontaneously developed a hypo-/hyper-pigmented skin phenotype on their tails (Fig. 2A and B; unpublished data), reminiscent of the hallmark skin feature of Type II RTS patients (20,26,28,29,32 and 33). In addition, 5.7% (18/314) of the homozygous mutant mice had skeletal defects of the limbs at birth, with most of these defects being preaxial polydactyly of the hind limbs (Fig. 2C and D). The incidence of polydactyly in $Recql4^{-/-}$ mice (15/314) differed significantly from controls (1/189; a single heterozygous mouse had preaxial polydactyly of the left hind limb; $P = 0.007$, $\chi^2 = 7.01$, Fisher's exact test). More severe limb defects such as reduction deficiency of the left arm were also observed (Fig. 2F). In addition, we also observed palatal patterning defects in all the mutant mice examined (50/50), but not in the controls (0/30). These defects varied in severity ranging from cleft palate (Fig. 2H) to subtle patterning defects (Fig. 2J). Palatal defects have not been recognized as a common feature for Type II RTS (26).

Recql4 deficiency modifies the multiplicity and size of intestinal adenomas in Apc^{min} mice

In humans, Type II RTS is associated with increased susceptibility to early-onset osteosarcoma (28). In a systematic analysis of 100 $Recql4^{-/-}$ mice and 43 $Recql4^{+/-}$ or $Recql4^{+/+}$ control mice, we found that five $Recql4^{-/-}$ mice and no $Recql4^{+/-}$ or $Recql4^{+/+}$ control mice died of cancer prior to 20 months of age. Among these five $Recql4^{-/-}$ mice that died of cancer, two had osteosarcoma and three developed lymphomas. The observed tumor incidence is not sufficient to determine whether there exists a significant difference in tumor susceptibility between $Recql4^{-/-}$ mice and wild-type controls. Thus, we bred the *Recql4* mutant mice with Apc^{min} mice (36). The Apc^{min} allele creates a sensitized background that is useful to evaluate the effect of specific genetic mutations on gastrointestinal tumor susceptibility in the mouse (37,38). Thus, we examined the effect of the *Recql4* deficiency on the susceptibility and progression of intestinal tumors in Apc^{min} mice either at 120 days, when macroadenomas in these mice can be readily scored, or at the time of their natural death.

At 120 days of age, we observed a 2-fold increase in the multiplicity of macroadenomas along the entire GI tract in $Recql4^{-/-}$, $Apc^{Min/+}$ when compared with $Recql4^{+/-}$ $Apc^{Min/+}$ mice (Fig. 3A; Table 1). In addition to developing more macroadenomas, the average maximal diameter of the macroadenomas was larger in $Recql4^{-/-}$, $Apc^{Min/+}$ when compared with $Recql4^{+/-}$, $Apc^{Min/+}$ mice (Fig. 3B; Table 1). Finally, the $Recql4^{-/-}$, $Apc^{Min/+}$ mice always developed tumors in the large intestine, a site that is inconsistently affected in $Recql4^{+/-}$, $Apc^{Min/+}$ mice or in $Recql4^{+/+}$, $Apc^{Min/+}$ mice (36).

At natural death, we observed no difference in the mean or maximal lifespan between $Recql4^{-/-}$, $Apc^{Min/+}$ and $Recql4^{+/-}$, $Apc^{Min/+}$ cohorts, despite dramatic increases in tumor load in the intestines of the $Recql4^{-/-}$, $Apc^{Min/+}$mice (Table 1). Remarkably, $Recql4^{-/-}$, $Apc^{Min/+}$ mice died with numerous tumors occupying the entire interior surface of the distal ileum, compared with fewer tumors in the same area in $Recql4^{+/-}$, $Apc^{Min/+}$ sibling mice (Fig. 3C and D). Despite the increase in number and size of tumors in $Recql4^{-/-}$, $Apc^{Min/+}$ mice, their histological grade did not differ from those of $Recql4^{+/-}$, $Apc^{Min/+}$ mice with respect to tumor invasiveness (data not shown). These data demonstrate that *Recql4* deficiency significantly modifies tumor susceptibility, but not tumor invasiveness in an $Apc^{Min/+}$ genetic background.

Aneuploidy in $Recql4^{-/-}$ cells

Chromosomal instability has been observed in cell lines derived from Type II RTS patients, suggesting that it may be a cellular feature of this syndrome (29,31–34). Therefore, we utilized cells from our mouse model to interrogate the nature of genomic instability in $Recql4^{-/-}$ cells. Chromosome analysis was carried out using primary mouse embryonic fibroblast (MEF) cultures of wild-type and $Recql4^{-/-}$ cells. At passage 2, wild-type cells displayed a stable, near-diploid mean number of chromosomes (39.5 ± 0.20 chromosomes/cell) with $<1\%$ aneuploid cells (Fig. 4A and C). In contrast, at the same passage, 24% of $Recql4^{-/-}$ cells were hyperploid and had an abnormal mean number of chromosomes (45.0 ± 2.25 chromosomes/cell; Fig. 4B and C). We also found that $Recql4^{-/-}$ MEFs had a significantly higher frequency of spontaneous micronuclei than their wild-type counterparts (two-factor ANOVA, $P < 0.001$ for all Bonferoni corrected null hypotheses, Fig. 4D). In addition to chromosome counts, each metaphase spread was screened for evidence of other types of chromosomal instability. We did not observe increased rates of sister-chromatid exchange (data not shown), multi-radial chromosomes, chromosome breakages or fusions. However, we noticed that in several spreads from $Recql4^{-/-}$ cells sister-chromatids of metaphase chromosomes were no longer associated with one another at their centromeric regions. These spreads were excluded from chromosome counts and analyzed in more detail in subsequent analysis.

To determine whether the aneuploidy phenotype was unique to MEFs or is a common feature of many $Recql4^{-/-}$ cells, we extended our chromosome analysis to include primary cells isolated from adult mice. We found that all cell types from $Recql4^{-/-}$ mice examined, including adult bone marrow, B- and T-cells, displayed higher rates of aneuploidy than wild-type controls (Fig. 4C). Thus, the aneuploidy phenotype appears to be a common feature of many, if not all $Recql4^{-/-}$ cell types.

Premature centromere separation in $Recql4^{-/-}$ cells

In mammalian cells, aneuploidy may arise through several mechanisms, including defective telomere metabolism,

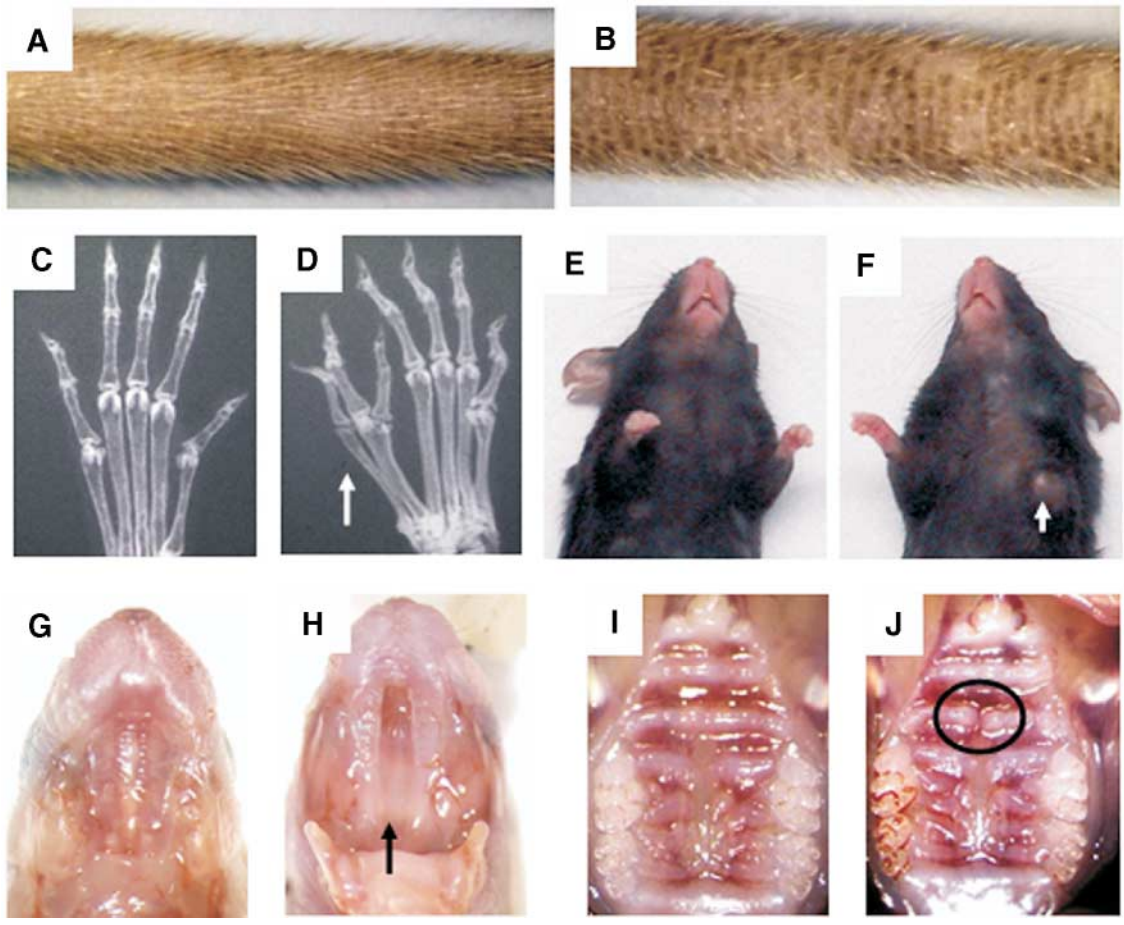

Figure 2. Major morphological phenotypes of *Recql4*$^{-/-}$ mice. Photographs of the tails of a wild-type mouse (**A**) and a *Recql4*$^{-/-}$ mouse (**B**) at 12 months of age. Note the striking hypo-/hyper-pigmented areas on the tail of the *Recql4*$^{-/-}$ mouse. (**C**–**F**) Radial ray defects in mice. X-ray radiographs of the hind limbs of an adult wild-type (C) and *Recql4* mutant (D) mouse. Note that the *Recql4*$^{-/-}$ mouse has an extra digit and a bifurcated digit of the hind limb (white arrow). Photographs of a wild-type mouse (E) and a *Recql4*$^{-/-}$ mouse (F) showing the truncated forelimb in the *Recql4*$^{-/-}$ mouse (white arrowhead). (**G**–**J**) Palatal photographs. Photographs of the palates of a wild-type (G) and a sibling *Recql4*$^{-/-}$ mouse (H) at postnatal day 1. Note the severe cleft palate in the mutant mouse (back arrow). Photographs of the palates of wild-type (I) and *Recql4*$^{-/-}$ (J) mice at 12 weeks of age. Note the patterning defect in the palate of the mutant mouse (denoted by a circle).

defective spindle checkpoint control and multi-polar spindles due to abnormal numbers of centrosomes (39). Thus, we systematically tested *Recql4*$^{-/-}$ MEFs for defects in each of these pathways. Observations on more than 1000 *Recql4*$^{-/-}$ metaphase spreads revealed no statistically significant increase in end-to-end fusions when compared with wild-type cells (data not shown), indicating that *Recql4*$^{-/-}$ cells have normal telomere metabolism. We then examined the response of cells to the microtubule-spindle poison Colcemid. We found that *Recql4*$^{-/-}$ cells accumulated mitoses and had similar mitotic indices to wild-type cells, indicating normal spindle checkpoint function in *Recql4*$^{-/-}$ MEFs (Fig. 5A). To test for centrosome defects, we performed immunostaining with anti-γ-tubulin antibodies and counterstained with DAPI. We found that the number of metaphase cells with greater than or equal to three centrosomes did not differ between *Recql4*$^{-/-}$ (1.6%) and wild-type (1.9%) cells (Fig. 5B, C and E). In contrast, *p53*$^{-/-}$ cells, which are known to have centrosome defects (40), had a much higher frequency of cells with greater than or equal to three centrosomes per cell (15.6%; Fig. 5D and E). Thus, none of these previously described mechanisms appears responsible for the aneuploid phenotype in *Recql4*$^{-/-}$ cells.

Premature centromere separation (PCS) refers to a situation in which sister-chromatids become precociously separated prior to the metaphase/anaphase transition (41). As noted earlier, we observed PCS in standard metaphase spreads from *Recql4*$^{-/-}$ MEF cells. To confirm the PCS phenotype, we first performed fluorescence *in situ* hybridization (FISH) experiments using two probes specific for chromosome 8 and chromosome 11. On a normal metaphase chromosome spread, a chromosome-specific FISH probe is expected to detect two pairs of signals with each pair representing targets on sister-chromatids. In contrast, on a chromosome after undergoing PCS, the probe would detect two separate unpaired signals. We found that this was the case in many

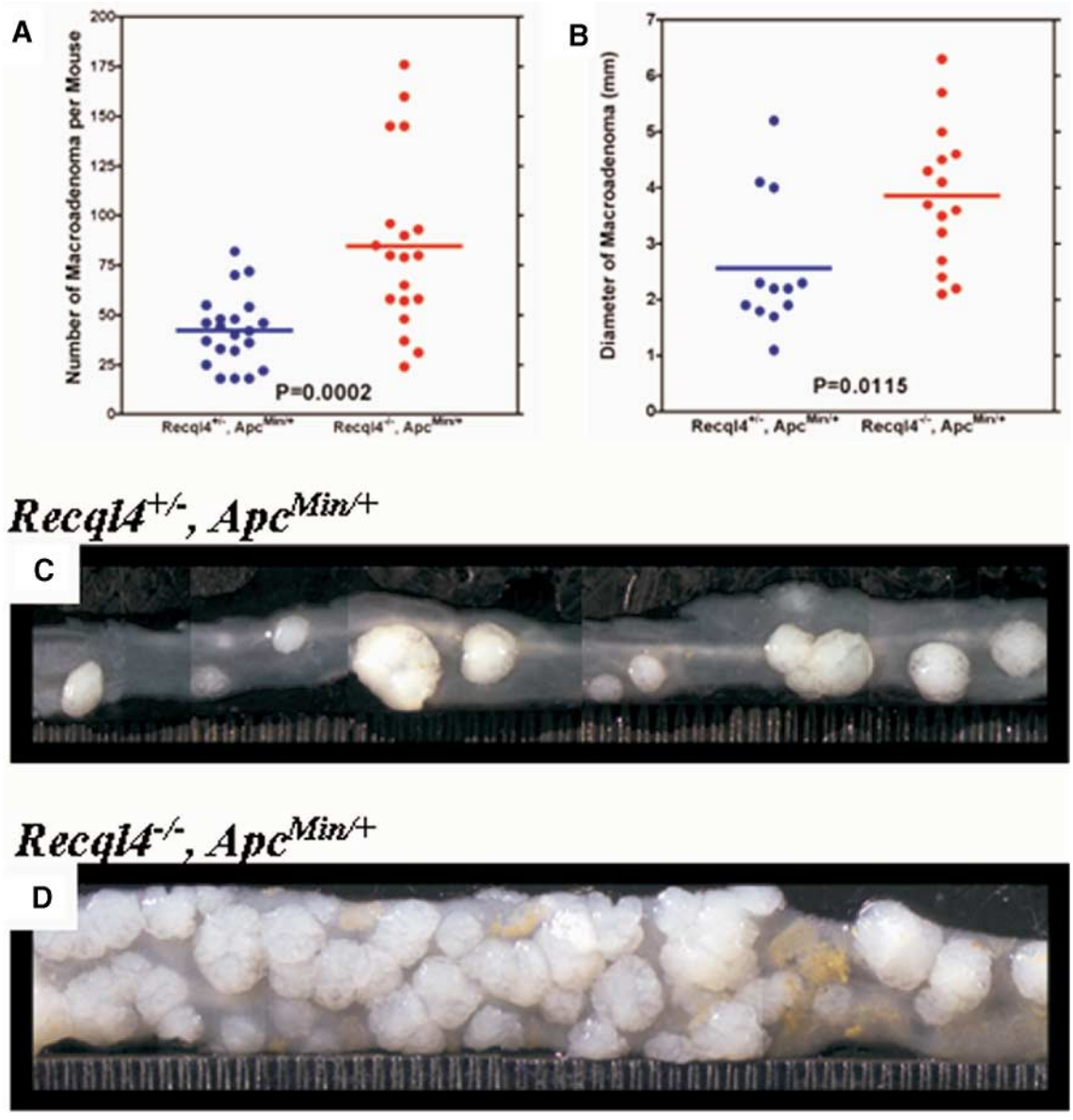

Figure 3. Multiplicity and size of adenomas in the mouse intestine. (**A** and **B**) Histograms showing tumor multiplicity and size from mice aged to 120 days. Each dot represents the number of tumors in the intestine of a single mouse and the horizontal line represents the mean of the population. (A) A histogram showing the tumor multiplicity in the intestines of $Recql4^{-/-}$, $Apc^{Min/+}$and $Recql4^{+/-}$, $Apc^{Min/+}$ mice. Note the significant 2-fold increase in the mean tumor multiplicity in $Recql4^{-/-}$, $Apc^{Min/+}$ mice when compared with $Recql4^{+/-}$, $Apc^{Min/+}$ mice. (B) A histogram showing the average maximal diameters of intestinal tumors at 120 days of age. Note the significant difference in the mean tumor size (denoted by horizontal lines) between $Recql4^{-/-}$, $Apc^{Min/+}$and $Recql4^{+/-}$, $Apc^{Min/+}$mice. (**C** and **D**) Photographs of tumors from the distal ilea of a $Recql4^{+/-}$, $Apc^{Min/+}$mouse (C) and its $Recql4^{-/-}$, $Apc^{Min/+}$sibling (D) at 6 months of age. Note the numerous tumors covering the interior surface of the intestine in the $Recql4^{-/-}$, $Apc^{Min/+}$mouse when compared with the fewer tumors in the same region in its $Recql4^{+/-}$, $Apc^{Min/+}$sibling.

of the $Recql4^{-/-}$ MEF cells (Fig. 6B and C). This observation confirmed our cytological diagnosis of PCS and excluded the possibility that we were counting tetraploid cells.

Subsequently, we systematically analyzed metaphase preparations from primary $Recql4^{-/-}$ and wild-type MEFs. The results demonstrated a significant increase in PCS in $Recql4^{-/-}$ MEFs when compared with wild-type MEFs (Fig. 6C). As PCS may occur in cultured mammalian cells subjected to prolonged treatment with spindle microtubule inhibitors (42), we confirmed that the increased frequency of PCS is an intrinsic property of $Recql4^{-/-}$ MEFs by measuring the incidence of PCS in metaphases from untreated, asynchronous MEF cultures (Fig. 6C). These results demonstrated a nearly 10-fold increase in PCS in $Recql4^{-/-}$ MEFs when compared with wild-type controls (7.5% versus 0.8%, respectively; Fig. 6C). Thus, *Recql4* deficiency leads to a significant increase in the frequency of PCS in MEFs.

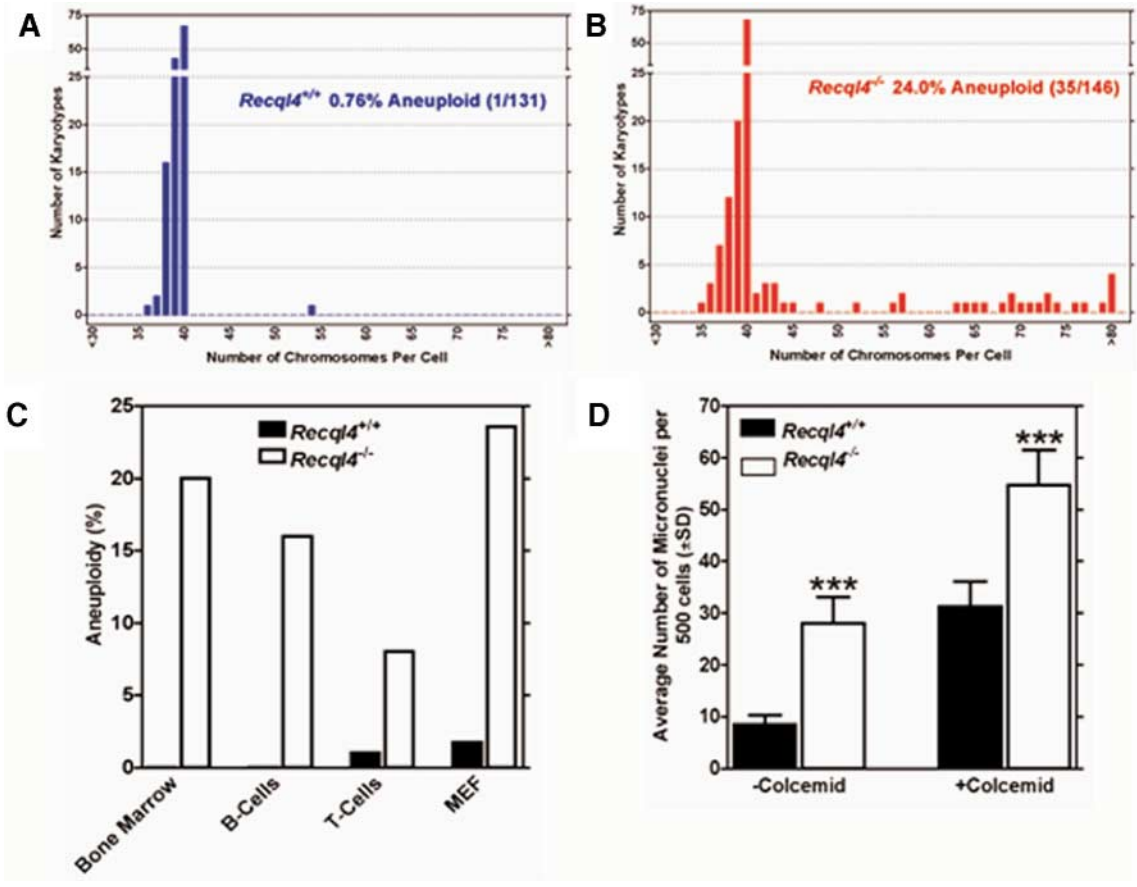

Figure 4. Aneuploidy and micronuclei in *Recql4*$^{-/-}$ cells. Chromosome analysis of DAPI stained chromosomes from wild-type (**A**) and *Recql4*$^{-/-}$ (**B**) MEF cells at passage 2 or 3. Note the dramatic increase of aneuploid cells and lack of significant numbers of tetraploid spreads from *Recql4*$^{-/-}$ MEFs. (**C**) Percentage of aneuploidy observed in different cell types. Bone marrow ($n = 80$), B- and T-cells ($n = 40$ each), MEF ($n = 230$). (**D**) Frequency of micronuclei in MEFs. Note the marked increase in the frequency of micronuclei in *Recql4*$^{-/-}$ MEFs both with the Colcemid treatment ($n = 2000$) and without ($n = 4000$). For each experiment, nuclei were examined in groups of 500 at a time.

Table 1. Effect of *Recql4* deficiency on macroadenoma multiplicity and size in *Apc*$^{Min/+}$ mice

Genotype class	Age (days)	Multiplicity (±SD) Entire intestine (*n*)	Large intestine (*n*)	Diameter (mm ± SD) Small intestine (*n*)	Large intestine (*n*)
Recql4$^{+/-}$, *Apc* $^{Min/+}$	120	42.2 ± 17.8 (21)	0.81 ± 0.93 (21)	1.7 ± 0.53 (71)	2.6 ± 1.2 (12)
Recql4$^{-/-}$, *Apc* $^{Min/+}$	120	84 ± 43.7 (19)***	2.05 ± 0.97 (19)*	2.2 ± 0.7 (37)***	3.9 ± 1.3 (15)*
Recql4$^{+/-}$, *Apc*$^{Min/+}$	194 ± 30[a]	76.7 ± 26.8 (12)	1.75 ± 2.4 (12)	2.6 ± 0.88 (92)	2.5 ± 0.91 (19)
Recql4$^{-/-}$, *Apc* $^{Min/+}$	180 ± 37[a]	124.4 ± 30.9 (15)***	3.9 ± 2.2 (15)*	3.0 ± 0.9 (195)***	3.6 ± 0.35 (22)**

*$P < 0.05$; **$P < 0.01$; ***$P < 0.001$; *n*, number of animals.
[a]Mean lifespan (±SD).

To determine whether the PCS phenotype is also a property of *Recql4*-deficient cells *in vivo*, we analyzed primary cells derived from adult mice. All cell types examined in *Recql4*$^{-/-}$ mice, including adult bone marrow, B-cells and T-cells, displayed a higher frequency of PCS than that observed in their control counterparts (Fig. 6C).

Taken together, these data demonstrate that the chromosomal instability and PCS phenotypes are present in all *Recql4*$^{-/-}$ cell types. As sister-chromatid cohesion is essential for normal mitotic chromosome segregation (9,10), our findings indicate that a cohesion defect contributes to the chromosomal instability in *Recql4*$^{-/-}$ cells.

DISCUSSION

Modeling Type II RTS using *Recql4* mutant mice

There have been prior attempts to model Type II RTS in the mouse by creating mutations in *Recql4* (43,44). However, these models have had limited success because of the lethality

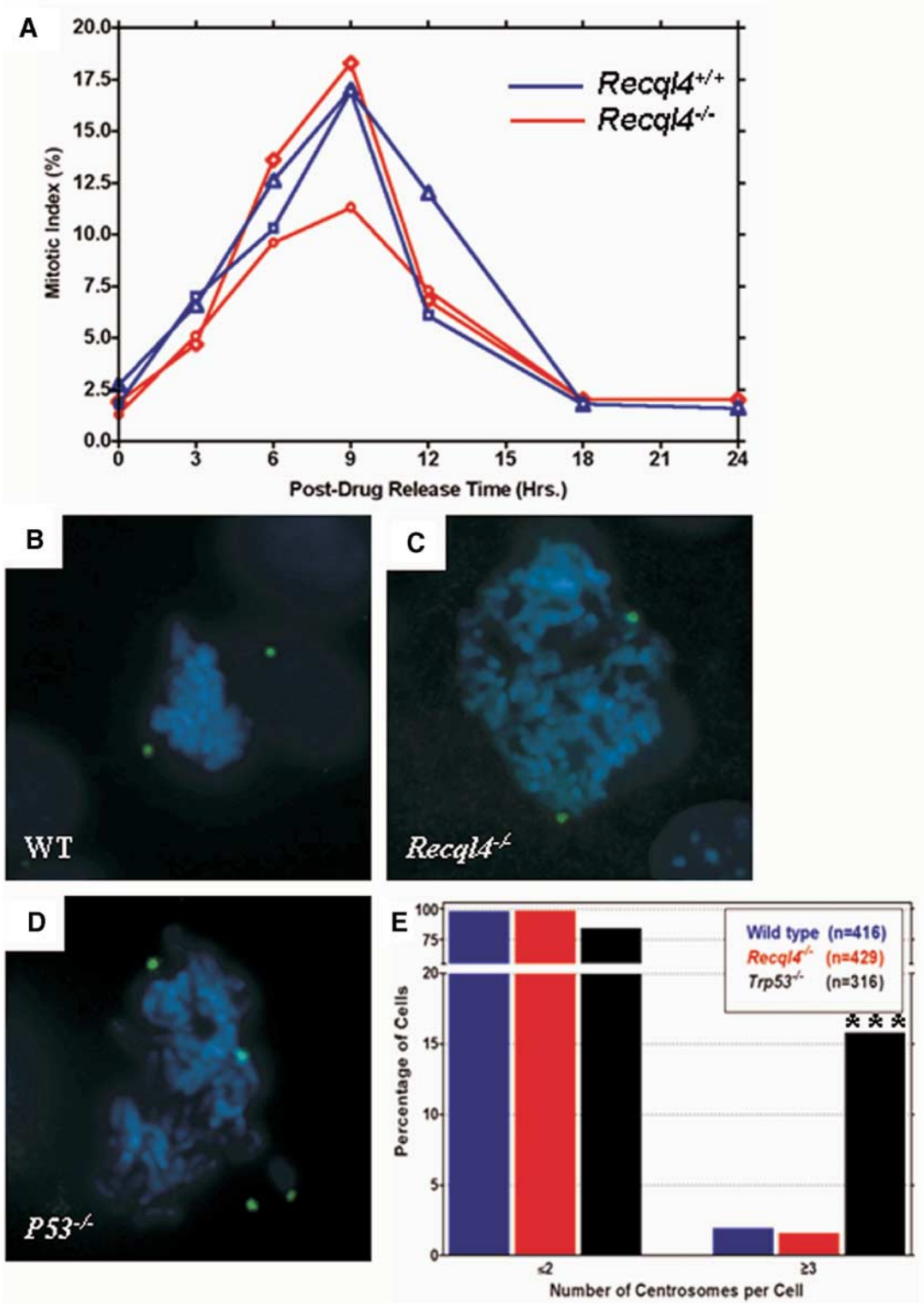

Figure 5. Mitotic indices and centrosome status in *Recql4*$^{-/-}$ MEFs. (**A**) Mitotic indices of wild type and *Recql4*$^{-/-}$ MEFs. Cells were treated with Colcemid, released and then harvested at different time points, stained with DAPI and analyzed by fluorecence microscopy. Note that both genotypes consistently respond to the spindle arrest in a similar manner. (**B**–**D**) Centrosome status in MEFs. Metaphase spreads were stained with anti-γ-tubulin (green) and counter-stained with DAPI (blue). (B) A representative metaphase spread of a normal diploid wild-type cell with a pair of centrosomes. (C) A representative metaphase spread of an aneuploid *Recql4*$^{-/-}$ cell with two centrosomes. (D) A representative metaphase spread of an aneuploid *p53*$^{-/-}$ cell with fours centrosomes. (**E**) Histogram showing the percentage of cells with no more than two (normal) or more than two (abnormal) centrosomes. Note the similarity between the wild-type and the *Recql4*$^{-/-}$ cells and the significantly higher frequency of cells with abnormal numbers of centrosomes in *p53*$^{-/-}$ cells (***$P < 0.0001$; Fisher's exact test).

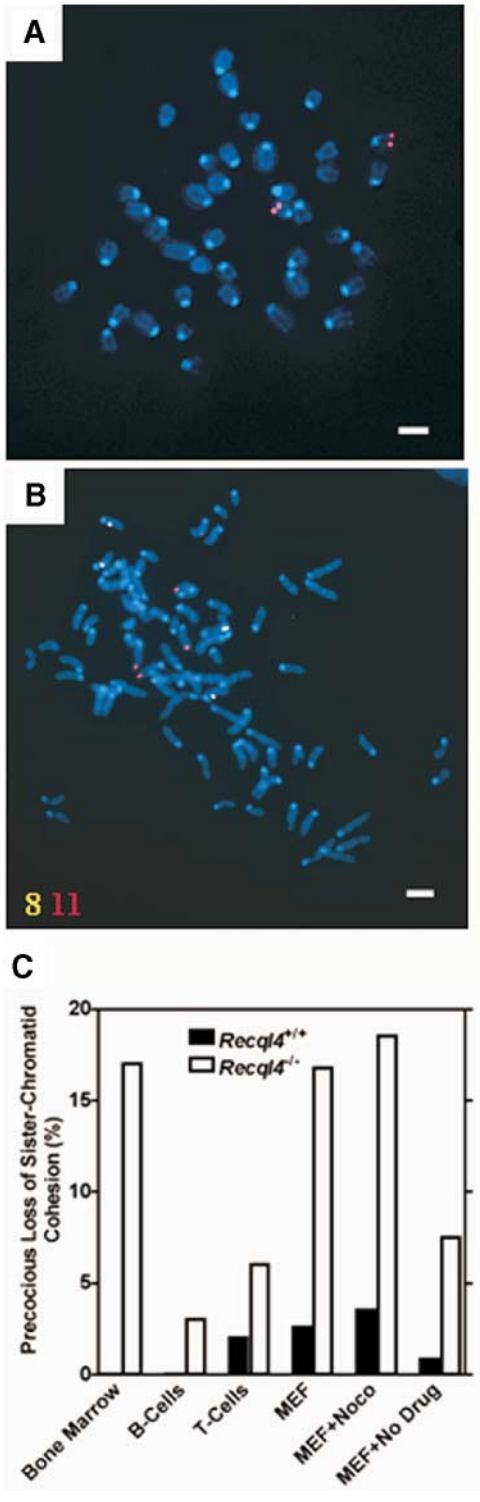

Figure 6. PCS in *Recql4*-deficeint cells. (**A** and **B**) Metaphase spreads prepared from Colcemid treated cells hybridized with probes specific for chromosome 8 (yellow) and chromosome 11 (red). Nuclear chromatin was stained with DAPI (blue). (A) A representative wild-type spread showing the distinct 'V' shaped chromosome indicative of the physical connection between the centromeres (centromeric cohesion) between sister-chromatids. Note that a chromosome 11 specific probe detects two pairs of signals (red). (B) A representative spread of a $Recql4^{-/-}$ cell in which the sister-chromatid cohesion no longer exists. Note the absence of the characteristic 'V' shaped mouse metaphase chromosomes with cohesive sister-chromatids. When the spread was hybridized with chromosome specific probes, each probe detects four unpaired signals (red for a chromosome 11 specific probe and yellow for a chromosome 8 specific probe, respectively), instead of two pairs of signals. Note the slight difference in the chromatid morphology between the two spreads. This reflects the general variation in chromatid morphology observed in FISH experiments, but is not a consistent difference between normal chromatids and those of *Recql4*-deficient cells. (**C**) Percentage of PCS observed in cells isolated from various sources. The standard Colcemid treatment was used in the preparation of the chromosome spreads for all cell types. However, for MEFs, spreads were also prepared in the absence of drug treatment (MEF + No Drug) and after treatment with Nocodazole (MEF + Noco), another spindle microtubule inhibitor. Note that for all cell types examined, the frequency of PCS is consistently much higher in the cells derived from the *Recql4* mutant mice than those from the wild-type controls, and in the case of MEFs, this is true regardless of the treatments used. Bone marrow ($n = 80$), B- and T-cells ($n = 60$ each), MEF-No Drug ($n = 120$), MEF-Colc ($n = 760$), MEF-Noco ($n = 600$). All scale bars represent 5 μM.

associated with these mutants (43,44). In contrast, the *Recql4* mutant mice reported here are viable, fertile and they recapitulate the major features of Type II RTS.

The reason for the discrepancy in phenotypes observed in the previous *Recql4* knockout models and in our model is not clear at present. In the first two models generated by Ichikawa *et al.*, (43) the mutant mice were embryonic lethal, whereas in the model generated by Hoki *et al.*, (44) only 5% of the mutant mice survived to 2 weeks of age (44). These observations raise the question of whether *Recql4* is essential for viability. Both our *Recql4* mutant allele and the one generated by Hoki *et al.* express aberrant *Recql4* transcripts that could potentially be translated into N-terminal truncated Recql4 polypeptide, a situation similar to many mutant alleles identified in Type II RTS patients. Although we have not been able to detect truncated polypeptide using currently available anti-Recql4 antibodies, this may reflect low sensitivity of the antibodies rather than absence of the protein. Therefore, it remains formally possible that our *Recql4* mutant allele and many of the *RECQL4* alleles identified in Type II RTS patients are hypomorphic alleles that retain some functions of RECQL4/Recql4 related to viability. Future experiments are needed to address this issue.

Interestingly, our *Recql4* model differs from the viable model generated by Hoki *et al.*. Hoki *et al.* (44) reported that their mutant mice had skin atrophy, colorless hair, hair loss, short stature, bone dysplasia, dystrophic teeth and immunological abnormalities. Importantly, their mice failed to develop poikiloderma and malignancies, both of which are hallmark features observed in Type II RTS patients (25–30). In contrast, the mutant mice reported here developed a pigmented skin feature reminiscent of poikiloderma (Fig. 2; unpublished data) and have increased cancer susceptibility in a sensitized Apc^{min} genetic background. Furthermore, our mutant mice had an increased incidence of limb defects and a chromosomal instability phenotype, two additional common features of Type II RTS that were not described in the report of Hoki *et al.* It should be stressed that the phenotypic differences between our *Recql4* knockout mice and those generated by Hoki *et al*. may reflect differences in the mutant *Recql4* alleles in these mice. Hoki *et al.* (44) replaced exon 13 with a *PGKneo* cassette, whereas we replaced exons 9 through 13 with a *PGKhprt* cassette. Thus, although both

alleles express aberrant *Recql4* transcript, only the allele generated by Hoki *et al.* expresses an aberrant transcript that could be translated into a polypeptide containing both the N- and C-terminal domains of Recql4.

Our observation of a complete penetrance palatal defect in our *Recql4* knockout mice is intriguing. Although the palatal patterning defects we observed have not previously been reported in Type II RTS (26), abnormal palates are a component feature of RAPADILINO syndrome (OMIM#266280) which is also caused by *RECQL4* mutations (45). In contrast to Type II RTS patients, RAPADILINO patients carry at least one copy of a founder hypomorphic *RECQL4* mutant allele (45). Future work is required to determine whether palatal patterning defects represent a common feature that is caused by *Recql4* or *RECQL4* deficiency in mice and humans, or a defect that is associated only with specific types of *Recql4* or *RECQL4* mutations. Intriguingly, another disorder exhibiting palatal defects may also be linked to *Recql4*; that is, in Roberts syndrome (RBS; OMIM no. 268300), a disorder characterized by a PCS phenotype in many cell types, patients exhibit congenital skeletal defects, including defects of the palate. The disease causing gene for this autosomal recessive genetic disorder has not been identified. Possibly, RBS is attributable to mutations in a gene that associates with RECQL4 or to an as yet unidentified mutation(s) in *RECQL4* itself.

Birth defects and genomic instability

The results from our study of *Recql4* mutant mice demonstrate a role for *Recql4* in development of the palate and the limbs. Although the developmental mechanism(s) for the abnormalities in $Recql4^{-/-}$ mice are not fully understood, we speculate that they are secondary to elevated rates of genomic instability. Such a supposition would be consistent with the extensive documentation in man and in experimental animal models linking genomic instability and the occurrence of birth defects, particularly palatal and radial-limb abnormalities. For example, exposure of fetuses to clastagenic compounds or ionizing radiation can induce genomic instability and result in cleft palate and radial-limb defects (46,47). In addition, similar patterns of birth defects have been observed in patients with other genetic disorders that are associated with chromosomal instability, including RBS, Fanconi anemia (OMIM no.227650), Nijmegen breakage syndrome (OMIM no. 251260) and immunodeficiency-centromeric instability-facial anomalies syndrome (OMIM no. 242860). The precise mechanism by which genomic instability affects patterning and growth of these systems remains to be elucidated.

Aneuploidy and cancer susceptibility

Our study demonstrates that *Recql4* deficiency in mice leads to elevated levels of aneuploidy and increased cancer susceptibility. We believe that aneuploidy is also the main genomic instability of Type II RTS, which is consistent with the increased chromosomal instability in cells derived from Type II RTS patients (29,31–34). An aneuploidy phenotype in Type II RTS is also consistent with a significant increase in susceptibility to early-onset osteosarcoma, which is well documented to involve chromosomal instability (48,49). Although *Recql4* deficiency alone is not sufficient to have a significant effect on the susceptibility to spontaneous osteosarcoma in mice, this may not be surprising. It is well documented that there are numerous intrinsic differences between mice and humans that can contribute to the differences in tumor susceptibilities between the two species. For example, there is a major difference in the lifespan and the total number of mitoses within the lifespan of mice and humans. Thus, it is possible that a specific genomic instability may have a major impact on cancer susceptibility in humans but not in mice. This is illustrated by the fact that specific mutant mouse strains that have genomic instability, but lack a significant increase in spontaneous cancer susceptibility (50,51). Importantly, we showed that *Recql4* deficiency led to a dramatic increase in the multiplicity and size of intestinal tumors in an Apc^{Min} tumor model, most notably in the large intestine, where the macroadenoma penetrance was increased from 50% in $Recql4^{+/-}$, $Apc^{Min/+}$ mice to 100% in $Recql4^{-/-}$, $Apc^{Min/+}$ mice. The effect of *Recql4* deficiency on tumorigenesis in the mouse intestine likely results from the chromosomal instability caused by *Recql4* deficiency, which would be consistent with the previous observations that link chromosomal instability to the etiology of gastrointestinal cancer in humans (52).

Given our observations of high rates of aneuploidy and PCS observed in all cell types examined in this study, we believe that these phenotypes represent a general feature of many, if not all, $Recql4^{-/-}$ cells. It is reasonable to assume that the fate of a given aneuploid cell may be different between the *in vitro* culture conditions and the *in vivo* micro-environments, and may vary among different cell types, thus accounting for the relatively lower frequency of aneuploidy in cells from *in vivo* tissues when compared with MEF cells grown in culture. On the basis of this assumption it is interesting to note that cancer susceptibility is limited to distinct tissue types in Type II RTS patients. The reasons for such tissue/organ specificity are not yet clear; however, it is reasonable to suggest that the cellular response to PCS may differ among cell types. Nonetheless, a link between cancer and increased PCS is well established in humans. Patients with other genetic disorders associated with PCS and aneuploidy, such as RBS and mosaic variegated aneuploidy syndrome (OMIM no. 257300), also show an increased cancer susceptibility (41,53,54).

Recql4 deficiency and chromosomal instability

The observation of a chromosome mis-segregation phenotype in budding yeast *sgs1Δ* mutants (12,13) provides direct genetic evidence for an important role for RecQ DNA helicase in modulating chromosome segregation. However, the mechanism(s) that lead to such a defect in *sgs1Δ* cells have not been experimentally defined. The common hyper-recombination phenotype observed in many *RecQ* mutants has led to the speculation that the failure of timely resolution of Holliday junctions may impede the dis-entanglement of sister chromatids and hence contribute to the chromosome segregation defects (55). We report here that *Recql4*

deficiency results in PCS and aneuploidy in a subset of *Recql4*$^{-/-}$ cells. We speculate that the chromosome mis-segregation phenotype of *sgs1Δ* mutants is caused by the same mechanism. Indeed, a recent study has provided genetic evidence for a link between *Sgs1* and *Ctf4*, a component of the cohesion establishment complex, and showed that the *sgs1Δ* mutants exhibited a PCS phenotype (56). Such conservation between yeast and mice may also suggest that a similar mechanism(s) is responsible for the chromosome instability observed in cells from Type II RTS patients (29,31–34). We have shown that *Recql4*$^{-/-}$ MEFs have normal frequency of sister-chromatid exchange (unpublished data), demonstrating that unlike its homologs Blm or Wrn, Recql4 does not have a significant role in regulating mitotic recombination. This finding sheds light on the apparent paradoxical notion that despite a high degree of similarity between BLM, WRN and RECQL4, their deficiency causes three clinically distinct syndromes. Our findings also indicate that in mammals, where five *RecQ* DNA helicase genes act in concert to maintain genomic stability, individual RecQ homologs have acquired specialized, non-redundant roles. In this context, genetic uncoupling of the functional roles related to recombination and chromosome segregation in mammals exists whereby regulation of the former is carried out by BLM and WRN and regulation of the latter is allocated to RECQL4.

The high rates of PCS and aneuploidy observed in all *Recql4*$^{-/-}$ cells examined suggest that this abnormality predisposes cells to aberrant mitosis and chromosome mis-segregation. It remains unclear exactly how Recql4 is involved in sister-chromatid cohesion. RECQL4 expression has been shown to be cell cycle regulated, with peak expression occurring during the G_1- and S-phases (57), coinciding with the timing of cohesion establishment (58). These data may suggest that Recql4/RECQL4 has a role in the establishment of cohesion during S-phase. Interestingly, it was recently reported that human RECQL4 physically interacts with UBR1 and UBR2 (59), two keys components of the N-end rule ubiquitination pathway (60), which has been shown to have an important role in controlling chromosome segregation in yeast (61). However, it remains unclear how, or whether, UBR1-RECQL4 or UBR2-RECQL4 interactions can affect sister-chromatid cohesion in mammalian cells. Finally, it should be noted that the majority of *Recql4*-deficient cells (75%) appear to establish the appropriate cohesion necessary for normal mitoses, suggesting that Recql4 may function as a regulator rather than as a component of the cohesion complex. Further work is required to experimentally elucidate how Recql4 helicase modulates sister-chromatid cohesion.

MATERIALS AND METHODS

Generation of *Recql4* knockout mice

To construct the replacement gene targeting vector *pRecQ4KO-tk*, a 4854 bp *Eco*RI/*Sau*AI fragment of the *Recql4* gene (accession AB042529) was cloned into pBluescript (*pBSSK*, Stragene, La Jolla, CA, USA). A 1.075 kb *Kpn*I/*Sac*I fragment (nucleotides 585–1660) was deleted and replaced with a *Kpn*I/*Sac*I digested *PGK-HPRT-mini* gene cassette (62). The *pRecQ4KO-tk* vector was linearized with *Sca*I, purified and electroporated into AB2.2 (129S7/SvEvBrd-Hprt$^{b\text{-}m2}$) mouse ES cells as described (63). Targeted clones were identified by screening HAT resistant colonies by Southern blotting using a 5′ external probe (5P in Fig. 1). This 5′ probe consisted of a 0.4 kb *Hin*dIII–*Eco*RI fragment which detects a 4.3 kb wild-type fragment and a 2.5 kb mutant fragment from *Hin*dIII digested genomic DNA. The 3′ probe consisted of a 0.35 kb *Bgl*II–*Hin*dIII restriction fragment which detects a 12 kb *Bam*HI fragment of the wild-type *Recql4* allele and an 8 kb *Bam*HI–*Eco*RV fragment of the targeted *Recql4* allele.

One of these correctly targeted ES cell clones, RecQ4KO.1, was expanded, purified and used to generate heterozygous *Recql4*^{tm1Glu} mutant mice as described (37). Briefly, chimeric males were mated with C57BL/6J (B6) females to obtain heterozygous mutant mice in a (B6x129S7/SvEvBrd-*Hprt*$^{b\text{-}m2}$) mixed genetic background. All *Recql4* mutant mice used in this study, unless otherwise specified, are in a mixed genetic background consisting of 75% B6 and 25% 129S7 genomes. Homozygous mutants were obtained by intercrossing heterozygous mice. The genotypes of all *Recql4* mutant mice were determined by Southern blotting.

RT–PCR analysis of *Recql4* expression

A pair of primers, Recql4.5ex8: 5′-AGAGCTACAGGTG CCTCATTG-3′ and Recql4.3ex15: 5′-CATGAAGGCCTG TTGTACTC-3′, corresponding to sequences in exon 8 and 15, respectively, were used to amplify a 981 bp fragment of *Recql4* cDNA. Total RNA was isolated from the testis of 6-week-old mice using TRIzol® (Invitrogen, Carlsbad, CA, USA) according to the instruction provided by the manufacturer. All RT–PCR reactions were carried out using Superscript™ II RT/Platinum® *Taq* mix (Invitrogen).

Mice

B6 and B6.*Apc*$^{Min/+}$ (*Min*) mice (36) were purchased from The Jackson Laboratory (Bar Harbor, ME, USA). Mice were maintained in an American Association of Laboratory Animals (AALAC) accredited barrier-free facility at Case Western Reserve University School of Medicine. Mice were fed (*ad libitum*) a commercially available rodent breeder diet, 5010 (PMI® LabDiet®, St Louis, MO, USA). All procedures were approved by the Case Western Reserve University Institutional Animal Care and Use Committee (IACUC).

Analysis of *Apc*$^{Min/+}$ mice

B6.129S5-*Recql4*$^{tm1Glu/tm1Glu}$ (F6N2) female mice and *Apc*$^{Min/+}$ male mice in a B6 background, both carry the B6 *Mom1* susceptibility allele *Pla2g2a*$^{S/S}$, were mated to generate *Recql4*$^{-/+}$, *Apc*$^{Min/+}$ progeny. These *Recql4*$^{-/+}$, *Apc*$^{Min/+}$ mice were then crossed to *Recql4*$^{-/-}$ females to obtain the experimental and control littermate animals. Genotyping of the *Apc*$^{+}$ and *Apc*^{Min} alleles was carried out by standard PCR methods available from The Jackson Laboratory website. For data at 120 days of age, *Recql4*$^{-/+}$, *Apc*$^{Min/+}$

and *Recql4*$^{-/-}$, *Apc*$^{Min/+}$ mice were euthanized by CO_2 asphyxiation for quantitative analysis of gastrointestinal adenomas. For data at natural death, *Recql4*$^{-/+}$, *Apc*$^{Min/+}$ and *Recql4*$^{-/-}$, *Apc*$^{Min/+}$ littermate mice were euthanized when they displayed overt symptoms of intestinal neoplasia and anemia, including rectal bleeding/prolapse, significant weight loss and progressive loss of color (whitening) of the snout and paws. The intestine was resected *en bloc*, washed in phosphate buffered saline (PBS), opened longitudinally and pinned luminal side up on black dissection wax. Intestinal adenomas (macroadenomas with maximal diameters $\geq$0.5 mm) along the entire intestine were counted by microscopic examination at 10× magnification followed by fixation with 10% formalin in PBS (Fisher Scientific, Fairlawn, NJ, USA). Digitized images of polyps and a metric ruler were captured using a SPOT software 3.2.5 for Macintosh™ and RT color SPOT camera mounted on a Leica MZFLIII workstation (Diagnostic Instruments, Inc., Sterling Heights, MI, USA). The images were imported into Adobe Photoshop 6.0 program where the ruler function was used to obtain the length of 1 mm from the ruler in each image. The measure of the largest average diameter per polyp was divided by the length of the 1 mm standard to determine polyp sizes. Statistical analyses were performed with the two-sample Student's *t*-test (normality tests for all data sets were $P > 0.05$) using the Prism 3 for Macintosh statistical package (GraphPad Software, Inc., San Diego, CA, USA).

Histopathologic analysis of tumors

Tumor tissues were fixed in 10% phosphate buffered formalin. Histological analysis was performed by standard methods. Sections of polyps (5–7 μm) stained with hematoxylin and eosin (H&E) were used to compare histological morphology.

Cell culture

Primary MEFs were generated from 13.5 day embryos by standard methods (64). The genotype of each MEF cell line was determined by Southern blotting. Cells were cultured at 37°C (5% CO_2) in Iscove's modified eagle's medium (IMEM) containing 10% fetal bovine serum (FBS), unless otherwise noted.

Chromosome analysis and FISH analysis

For cytogenetic assays, rapidly growing, passage 2 MEFs were treated with Colcemid (at a working concentration of 0.03–0.05 μg/ml) for 4 h and processed using standard cytogenetic procedures. Briefly, cells were washed with 1× PBS, trypsinized, incubated in 0.075 M KCl hypotonic solution at 37°C for 10 min, followed by fixation in 3 : 1 methanol–acetic acid. Cell suspensions were dropped onto freshly prepared slides and stained with Vectashield® Hardset™ mounting medium with DAPI (Vector Laboratories, Inc., Burlingame, CA, USA). Images were captured on a Zeiss Axiophot upright microscope with Photometrics Sensys CCD camera and the Quips Genetic Workstation software.

Bone marrow cells were isolated from the femur, tibia and pelvis of 6-week-old male wild-type and *Recql4*$^{-/-}$ littermate mice using RPMI-1640 supplemented with 10% FBS and 10 U/ml heparin. B- and T-cells were isolated from spleen and thymus, respectively, of 4–6 week old mice. For B-cells, four to six spleens of the same genotypes were pooled to create a single cell suspension. The cells were then incubated in RPMI-1640 containing 10% FBS, 2 mM L-glutamine, 1 mM sodium pyruvate and 2 × P/S for 48 h followed by a 4 h incubation in the presence of Colcemid. For T-cells, single cell suspensions were incubated in RPMI-1640 containing 10% FBS and Colcemid for 30 min. Spreads were prepared and analyzed as described above.

For FISH experiments, fluorescent DNA probes were prepared using bacterial artificial chromosomes (BACs) specific for chromosomes 8 (*Wrn*) and 11 (*Brca1*), respectively, using the SpectrumGreen™ or SpectrumRed™ direct-labeled dUTP by nick translation as per the manufactures instructions (VYSIS, Inc., Downers Grove, IL, USA). These probes were then used to hybridize to fixed nuclei as described (65). After the hybridization, nuclear chromatin was counterstained with DAPI.

ACKNOWLEDGEMENTS

The authors wish to thank Pat Hunt, Matt Warman and Karen Mann for helpful comments on the manuscript and Josh Friedman, Youngji Park and Cheryl Urban for technical assistance. G.L. also wishes to thank Dr Allan Bradley for his generous support during the course of this study. This work was supported by grants from the National Cancer Institute (CA 89391) and The March of Dimes (5-FY00-570) to G.L. M.B.M. is supported by an NIH predoctoral fellowship to the Department of Genetics (5T32GM008613-08).

REFERENCES

1. Duesberg, P. and Rasnick, D. (2000) Aneuploidy, the somatic mutation that makes cancer a species of its own. *Cell Motil. Cytoskeleton*, **47**, 81–107.
2. Gebhart, E. and Liehr, T. (2000) Patterns of genomic imbalances in human solid tumors (Review). *Int. J. Oncol.*, **16**, 383–399.
3. Lengauer, C., Kinzler, K.W. and Vogelstein, B. (1998) Genetic instabilities in human cancers. *Nature*, **396**, 643–649.
4. Mertens, F., Johansson, B., Hoglund, M. and Mitelman, F. (1997) Chromosomal imbalance maps of malignant solid tumors: a cytogenetic survey of 3185 neoplasms. *Cancer Res.*, **57**, 2765–2780.
5. Nicklas, R.B. (1997) How cells get the right chromosomes. *Science*, **275**, 632–637.
6. Nicklas, R.B. and Koch, C.A. (1969) Chromosome micromanipulation. 3. Spindle fiber tension and the reorientation of mal-oriented chromosomes. *J. Cell Biol.*, **43**, 40–50.
7. Rieder, C.L. and Salmon, E.D. (1998) The vertebrate cell kinetochore and its roles during mitosis. *Trends Cell Biol.*, **8**, 310–318.
8. Nasmyth, K. (2002) Segregating sister genomes: the molecular biology of chromosome separation. *Science*, **297**, 559–565.
9. Uhlmann, F. (2001) Chromosome cohesion and segregation in mitosis and meiosis. *Curr Opin. Cell Biol.*, **13**, 754–761.
10. Cleveland, D.W., Mao, Y. and Sullivan, K.F. (2003) Centromeres and kinetochores: from epigenetics to mitotic checkpoint signaling. *Cell*, **112**, 407–421.
11. Hickson, I.D. (2003) RecQ helicases: caretakers of the genome. *Nat. Rev. Cancer*, **3**, 169–178.
12. Watt, P.M., Louis, E.J., Borts, R.H. and Hickson, I.D. (1995) Sgs1: a eukaryotic homolog of *E. coli* RecQ that interacts with topoisomerase II *in vivo* and is required for faithful chromosome segregation. *Cell*, **81**, 253–260.

13. Watt, P.M., Hickson, I.D., Borts, R.H. and Louis, E.J. (1996) SGS1, a homologue of the Bloom's and Werner's syndrome genes, is required for maintenance of genome stability in *Saccharomyces cerevisiae*. *Genetics*, **144**, 935–945.
14. Stewart, E., Chapman, C.R., Al-Khodairy, F., Carr, A.M. and Enoch, T. (1997) rqh1+, A fission yeast gene related to the Bloom's and Werner's syndrome genes, is required for reversible S phase arrest. *EMBO J.*, **16**, 2682–2692.
15. Gangloff, S., McDonald, J.P., Bendixen, C., Arthur, L. and Rothstein, R. (1994) The yeast type I topoisomerase Top3 interacts with Sgs1, a DNA helicase homolog: a potential eukaryotic reverse gyrase. *Mol. Cell. Biol.*, **14**, 8391–8398.
16. Ahmad, F., Kaplan, C.D. and Stewart, E. (2002) Helicase activity is only partially required for *Schizosaccharomyces pombe* Rqh1p function. *Yeast*, **19**, 1381–1398.
17. Kitao, S., Ohsugi, I., Ichikawa, K., Goto, M., Furuichi, Y. and Shimamoto, A. (1998) Cloning of two new human helicase genes of the RecQ family: biological significance of multiple species in higher eukaryotes. *Genomics*, **54**, 443–452.
18. Kitao, S., Lindor, N.M., Shiratori, M., Furuichi, Y. and Shimamoto, A. (1999) Rothmund–Thomson syndrome responsible gene, *RECQL4*: genomic structure and products. *Genomics*, **61**, 268–276.
19. Ellis, N.A., Groden, J., Ye, T.Z., Straughen, J., Lennon, D.J., Ciocci, S., Proytcheva, M. and German, J. (1995) The Bloom's syndrome gene product is homologous to RecQ helicases. *Cell*, **83**, 655–666.
20. Kitao, S., Shimamoto, A., Goto, M., Miller, R.W., Smithson, W.A., Lindor, N.M. and Furuichi, Y. (1999) Mutations in RECQL4 cause a subset of cases of Rothmund–Thomson syndrome. *Nat. Genet.*, **22**, 82–84.
21. Yu, C.E., Oshima, J., Fu, Y.H., Wijsman, E.M., Hisama, F., Alisch, R., Matthews, S., Nakura, J., Miki, T., Ouais, S. *et al.* (1996) Positional cloning of the Werner's syndrome gene. *Science*, **272**, 258–262.
22. Fukuchi, K., Martin, G.M. and Monnat, R.J., Jr (1989) Mutator phenotype of Werner syndrome is characterized by extensive deletions. *Proc. Natl Acad. Sci. USA* **86**, 5893–5897.
23. Goto, M., Miller, R.W., Ishikawa, Y. and Sugano, H. (1996) Excess of rare cancers in Werner syndrome (adult progeria). *Cancer Epidemiol. Biomarkers Prev.*, **5**, 239–246.
24. German, J. (1993) Bloom syndrome: a mendelian prototype of somatic mutational disease. *Medicine (Baltimore)*, **72**, 393–406.
25. Vennos, E.M. and James, W.D. (1995) Rothmund–Thomson syndrome. *Dermatol. Clin.*, **13**, 143–150.
26. Wang, L.L., Levy, M.L., Lewis, R.A., Chintagumpala, M.M., Lev, D., Rogers, M. and Plon, S.E. (2001) Clinical manifestations in a cohort of 41 Rothmund–Thomson syndrome patients. *Am. J. Med. Genet.*, **102**, 11–17.
27. Kerr, B., Ashcroft, G.S., Scott, D., Horan, M.A., Ferguson, M.W. and Donnai, D. (1996) Rothmund–Thomson syndrome: two case reports show heterogeneous cutaneous abnormalities, an association with genetically programmed ageing changes, and increased chromosomal radiosensitivity. *J. Med. Genet.*, **33**, 928–934.
28. Wang, L.L., Gannavarapu, A., Kozinetz, C.A., Levy, M.L., Lewis, R.A., Chintagumpala, M.M., Ruiz-Maldanado, R., Contreras-Ruiz, J., Cunniff, C., Erickson, R.P. *et al.* (2003) Association between osteosarcoma and deleterious mutations in the *RECQL4* gene in Rothmund–Thomson syndrome. *J. Natl Cancer Inst.*, **95**, 669–674.
29. Lindor, N.M., Furuichi, Y., Kitao, S., Shimamoto, A., Arndt, C. and Jalal, S. (2000) Rothmund–Thomson syndrome due to RECQ4 helicase mutations: report and clinical and molecular comparisons with Bloom syndrome and Werner syndrome. *Am. J. Med. Genet.*, **90**, 223–228.
30. Pujol, L.A., Erickson, R.P., Heidenreich, R.A. and Cunniff, C. (2000) Variable presentation of Rothmund–Thomson syndrome. *Am. J. Med. Genet.*, **95**, 204–207.
31. Balraj, P., Concannon, P., Jamal, R., Beghini, A., Hoe, T.S., Khoo, A.S. and Volpi, L. (2002) An unusual mutation in *RECQ4* gene leading to Rothmund–Thomson syndrome. *Mutat. Res.*, **508**, 99–105.
32. Beghini, A., Castorina, P., Roversi, G., Modiano, P. and Larizza, L. (2003) RNA processing defects of the helicase gene *RECQL4* in a compound heterozygous Rothmund–Thomson patient. *Am. J. Med. Genet.*, **120A**, 395–399.
33. Durand, F., Castorina, P., Morant, C., Delobel, B., Barouk, E. and Modiano, P. (2002) Rothmund–Thomson syndrome, trisomy 8 mosaicism and *RECQ4* gene mutation. *Ann. Dermatol. Venereol.*, **129**, 892–895.
34. Miozzo, M., Castorina, P., Riva, P., Dalpra, L., Fuhrman Conti, A.M., Volpi, L., Hoe, T.S., Khoo, A., Wiegant, J., Rosenberg, C. *et al.* (1998) Chromosomal instability in fibroblasts and mesenchymal tumors from 2 sibs with Rothmund–Thomson syndrome. *Int. J. Cancer*, **77**, 504–510.
35. Ohhata, T., Araki, R., Fukumura, R., Kuroiwa, A., Matsuda, Y., Tatsumi, K. and Abe, M. (2000) Cloning, genomic structure and chromosomal localization of the gene encoding mouse DNA helicase RecQ helicase protein-like 4. *Gene*, **261**, 251–258.
36. Moser, A.R., Pitot, H.C. and Dove, W.F. (1990) A dominant mutation that predisposes to multiple intestinal neoplasia in the mouse. *Science*, **247**, 322–324.
37. Luo, G., Santoro, I.M., McDaniel, L.D., Nishijima, I., Mills, M., Youssoufian, H., Vogel, H., Schultz, R.A. and Bradley, A. (2000) Cancer predisposition caused by elevated mitotic recombination in Bloom mice. *Nat. Genet.*, **26**, 424–429.
38. Rudolph, K.L., Millard, M., Bosenberg, M.W. and DePinho, R.A. (2001) Telomere dysfunction and evolution of intestinal carcinoma in mice and humans. *Nat. Genet.*, **28**, 155–159.
39. Storchova, Z. and Pellman, D. (2004) From polyploidy to aneuploidy, genome instability and cancer. *Nat. Rev. Mol. Cell Biol.*, **5**, 45–54.
40. Fukasawa, K., Choi, T., Kuriyama, R., Rulong, S. and Vande Woude, G.F. (1996) Abnormal centrosome amplification in the absence of p53. *Science*, **271**, 1744–1747.
41. Parry, D.M., Mulvihill, J.J., Tsai, S.E., Kaiser-Kupfer, M.I. and Cowan, J.M. (1986) SC phocomelia syndrome, premature centromere separation, and congenital cranial nerve paralysis in two sisters, one with malignant melanoma. *Am. J. Med. Genet.*, **24**, 653–672.
42. Chamla, Y., Roumy, M., Lassegues, M. and Battin, J. (1980) Altered sensitivity to cholchicine and PHA in human cultured cells. *Hum. Genet.*, **53**, 249–253.
43. Ichikawa, K., Noda, T. and Furuichi, Y. (2002) Preparation of the gene targeted knockout mice for human premature aging diseases, Werner syndrome, and Rothmund–Thomson syndrome caused by the mutation of DNA helicases. *Nippon Yakurigaku Zasshi*, **119**, 219–226.
44. Hoki, Y., Araki, R., Fujimori, A., Ohhata, T., Koseki, H., Fukumura, R., Nakamura, M., Takahashi, H., Noda, Y., Kito, S. *et al.* (2003) Growth retardation and skin abnormalities of the Recql4-deficient mouse. *Hum. Mol. Genet.*, **12**, 2293–2299.
45. Siitonen, H.A., Kopra, O., Kaariainen, H., Haravuori, H., Winter, R.M., Saamanen, A.M., Peltonen, L. and Kestila, M. (2003) Molecular defect of the Rapadilino syndrome expands the phenotype spectrum of Recql diseases. *Hum. Mol. Genet.*, **21**, 2837–2844.
46. Nomura, M., Suzuki, M., Suzuki, Y., Ikeda, H., Tamura, J., Koike, M., Jie, T. and Itoh, G. (1996) Cyclophosphamide-induced apoptosis induces phocomelia in the mouse. *Arch. Toxicol.*, **70**, 672–677.
47. Liang, L., Shao, C., Deng, L., Mendonca, M.S., Stambrook, P.J. and Tischfield, J.A. (2002) Radiation-induced genetic instability *in vivo* depends on p53 status. *Mutat. Res.*, **502**, 69–80.
48. Hiddemann, W., Roessner, A., Wormann, B., Mellin, W., Klockenkemper, B., Bosing, T., Buchner, T. and Grundmann, E. (1987) Tumor heterogeneity in osteosarcoma as identified by flow cytometry. *Cancer*, **59**, 324–328.
49. Bauer, H.C., Kreicbergs, A., Silfversward, C. and Tribukait, B. (1988) DNA analysis in the differential diagnosis of osteosarcoma. *Cancer*, **61**, 2532–2540.
50. Hollander, M.C., Sheikh, M.S., Bulavin, D.V., Lundgren, K., Augeri-Henmueller, L., Shehee, R., Molinaro, T.A., Kim, K.E., Tolosa, E., Ashwell, J.D. *et al.* (1999) Genomic instability in Gadd45a-deficient mice. *Nat. Genet.*, **23**, 176–184.
51. Celeste, A., Difilippantonio, S., Difilippantonio, M.J., Fernandez-Capetillo, O., Pilch, D.R., Sedelnikova, O.A., Eckhaus, M., Ried, T., Bonner, W.M. and Nussenzweig, A. (2003) H2AX haploinsufficiency modifies genomic stability and tumor susceptibility. *Cell*, **114**, 371–383.
52. Lengauer, C., Kinzler, K.W. and Vogelstein, B. (1997) Genetic instability in colorectal cancers. *Nature*, **386**, 623–627.
53. Plaja, A., Mediano, C., Cano, L., Vendrell, T., Sarret, E., Farran, I. and Sanchez, M.A. (2003) Prenatal diagnosis of a rare chromosomal instability syndrome: variegated aneuploidy related to premature centromere division (PCD). *Am. J. Med. Genet.*, **117A**, 85–86.
54. Kajii, T., Kawai, T., Takumi, T., Misu, H., Mabuchi, O., Takahashi, Y., Tachino, M., Nihei, F. and Ikeuchi, T. (1998) Mosaic variegated aneuploidy with multiple congenital abnormalities: homozygosity for total premature chromatid separation trait. *Am. J. Med. Genet.*, **78**, 245–249.

55. Wu, L. and Hickson, I.D. (2002) RecQ helicases and cellular responses to DNA damage. *Mutat. Res.*, **509**, 35–47.
56. Warren, C.D., Eckley, D.M., Lee, M.S., Hanna, J.S., Hughes, A., Peyser, B., Jie, C., Irizarry, R. and Spencer, F.A. (2004) S-phase checkpoint genes safeguard high-fidelity sister chromatid cohesion. *Mol. Biol. Cell.*, **15**, 1724–1735.
57. Kawabe, T., Tsuyama, N., Kitao, S., Nishikawa, K., Shimamoto, A., Shiratori, M., Matsumoto, T., Anno, K., Sato, T., Mitsui, Y. *et al.* (2000) Differential regulation of human RecQ family helicases in cell transformation and cell cycle. *Oncogene*, **19**, 4764–4772.
58. Uhlmann, F. and Nasmyth, K. (1998) Cohesion between sister chromatids must be established during DNA replication. *Curr. Biol.*, **8**, 1095–1101.
59. Yin, J., Tae Kwon, Y., Varshavsky, A. and Wang, W. (2004) RECQL4, mutated in the Rothmund–Thomson and RAPADILINO syndromes, interacts with ubiquitin ligases UBR1 and UBR2 of the N-end rule pathway. *Hum. Mol. Genet.*, **13**, 2421–2430.
60. Bachmair, A., Finley, D. and Varshavsky, A. (1986) *In vivo* half-life of a protein is a function of its amino-terminal residue. *Science*, **234**, 179–186.
61. Rao, H., Uhlmann, F., Nasmyth, K. and Varshavsky, A. (2001) Degradation of a cohesin subunit by the N-end rule pathway is essential for chromosome stability. *Nature*, **410**, 955–959.
62. Dong, J., Albertini, D.F., Nishimori, K., Kumar, T.R., Lu, N. and Matzuk, M.M. (1996) Growth differentiation factor-9 is required during early ovarian folliculogenesis. *Nature*, **383**, 531–535.
63. Ramirez-Solis, R., Davis, A.C. and Bradley, A. (1993) Gene targeting in embryonic stem cells. *Methods Enzymol.*, **225**, 855–878.
64. Hogan, B., Beddington, R., Costantini, F. and Lacey, E. (1994) *Manipulating the Mouse Embryo: A Laboratory Manual*, 2nd edn. Cold Spring Harbor Laboratory Press, Cold Spring Harbor, NY.
65. Van Stedum, S. and King, W. (2002) Basic FISH techniques and troubleshooting. *Methods Mol. Biol.*, **204**, 51–63.